Forschung im Ingenieurwesen (2025)89:118
https://doi.org/10.1007/s10010-025-00885-0

ORIGINALARBEITEN/ORIGINALS

Experimental investigation of the influence of axis misalignments in stepped planetary gear stages on the excitation and displacement behavior

Maximilian Stary[1] · Christian Westphal[1,2] · Christian Brecher[1,3]

Received: 7 April 2025 / Accepted: 1 August 2025

Abstract

With the increasing electrification of vehicles, the demand for suitable transmission concepts is growing. The high volume and weight of batteries require savings in other areas. Furthermore, due to the differing output characteristic curves of electric motors, shiftable transmissions are often unnecessary. Instead, a single gear transmission is sufficient. High-speed electric motors offer a weight advantage due to lower torques, which creates a need for especially high transmission ratios. Stepped planetary gearboxes meet these requirements while also delivering high power density. The elimination of masking noises from the combustion engine further highlights the acoustics of the transmission. Consequently, excitation behavior is increasingly seen as a quality criterion. The excitation behavior of planetary gear systems has already been the subject of numerous research studies. In contrast, there are only a few investigations regarding stepped planetary gear systems. Previous simulation studies indicate that stepped planetary gearboxes are sensitive to axis misalignments [1]. However, sufficient experimental results are not yet available. This paper presents the results of investigations conducted on a stepped planetary gearbox test rig with a sequential mesh sequence in both the sun-planet and planet-ring gear contact and a floating sun. The measurement setup allows the investigation of transmission error, structure-borne noise, and displacement of the sun gear shaft and the planet carrier. Using eccentric bushings, defined misalignment states can be imposed on the otherwise rigid gearbox. This enables the investigation of the influence of axis misalignments of the stepped planets and the carrier on the excitation and dynamic displacement behavior.

The investigations show frequency and amplitude modulations that had previously only been observed in planetary gear systems. Additionally, long-wavelength excitations in the range of the rotational frequencies of the shafts were identified, occurring either exclusively in the transmission error or in the structure-borne noise. The displacement behavior is analyzed based on the sun gear trajectory. A trochoidal path of the sun gear can be seen. The loops superimposed on the circular sun trajectory can be attributed to geometric deviations in the gears. The investigations demonstrate that planet pin position errors have the greatest influence on the sun gear trajectory. For these cases, it is shown that the sun gear is deflected by the reaction forces from the tooth contacts until a load balance is established.

1 Motivation and introduction

With the increasing electrification of vehicles, the demand for suitable transmission concepts is also growing [2]. The large volume and weight of batteries require compensations in other areas [3]. Moreover, electric motors can often operate without variable gear ratios due to their torque-speed characteristics, which differ from those of internal combustion engines [4]. In many cases, a single gear reduction or increase stage is sufficient [2]. Especially high-speed electric motors offer a weight advantage, which in turn requires particularly high transmission ratios [5]. Stepped planetary gearboxes meet these requirements by extending the ad-

✉ Maximilian Stary
m.stary@wzl.rwth-aachen.de

[1] Werkzeugmaschinenlabor WZL der RWTH Aachen University, Campus-Boulevard 30, 52074 Aachen, Germany

[2] Manufacturing Technology Institute MTI der RWTH Aachen University, Campus-Boulevard 30, 52074 Aachen, Germany

[3] Fraunhofer-Institut für Produktionstechnologie IPT, Steinbachstraße 17, 52074 Aachen, Germany

Published online: 29 August 2025

vantages of conventional planetary gear systems with an additional gear stage [6].

With the elimination of the masking noise from combustion engines, the acoustic behavior of the transmission becomes increasingly relevant. As a result, excitation behavior is becoming an important quality feature and should therefore be considered in the design process [7]. In stepped planetary gearboxes, the vibration behavior is significantly more complex than in conventional cylindrical gear systems. The multiple meshing contacts lead to additional interactions that must be accounted for during the design [6].

To further increase power density, material usage is minimized, with the gearbox housing in particular offering substantial savings potential. This results in a more elastic gearbox environment and leads to additional shaft displacements in the gear contact [8]. In stepped planetary gearboxes, tolerances and displacement behavior are often determined based on experience. While planetary gear systems have already been extensively studied, there are only a few investigations regarding the influence of axis misalignments in stepped planetary gearboxes [1, 9, 10]. Experimental studies on the impact of axis misalignments on the excitation behavior in stepped planetary gearboxes are still lacking. Test bench investigations can contribute to an enhanced understanding of the system and serve as a basis for the validation of simulation models.

2 State of the art

Stepped planetary gearboxes include various configurations of planetary gear systems in which the individual planets are replaced by stepped planets. This means that instead of a single gear, two gears are mounted on each planet shaft, see Fig. 1 left. Each of these gears meshes with one of the two central gears. The sun gear engages with the larger planet in the first stage, while the ring gear meshes with the smaller planet in the second stage. This configuration allows for an extended transmission ratio range while preserving the advantages of conventional planetary gear systems yet introduces additional complexity in its operational behavior. Due to the different numbers of teeth of the two planets of a stepped planet, a transmission ratio of up to $i_{total} = 20$ between the sun gear and the carrier is possible with a stationary ring gear [6].

The resulting power flow is shown on the right side of Fig. 1, where the power is split at the sun gear and recombined at the planet carrier. Manufacturing and assembly deviations can result in an imbalanced power distribution among the individual stepped planets. These load imbalances are of great importance to the operational behavior of the system [6]. In this paper, the excitation and displacement behavior of a stepped planetary gearbox is investigated experimentally. Therefore, the following section addresses the specific characteristics of stepped planetary gear systems in this context.

2.1 Excitation behavior of stepped planetary gear stages

Both transmission error and structure-borne noise are commonly used to evaluate the excitation behavior of cylindrical gears and have been validated through both simulation and experimental studies. In single-stage cylindrical gear systems, bearing force and moment excitation are directly

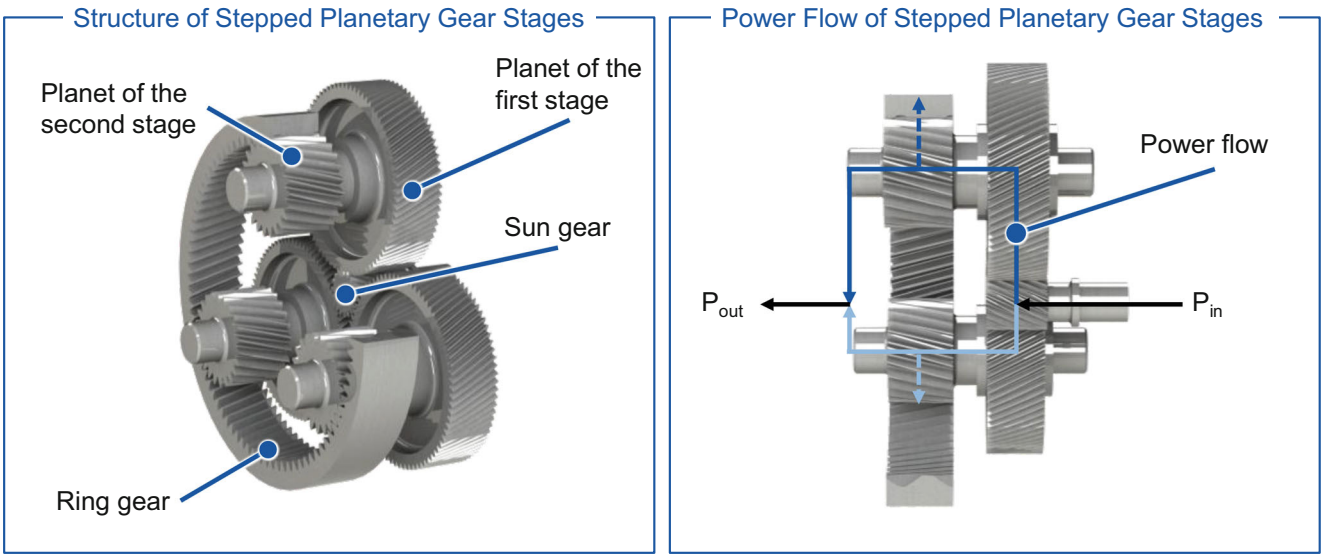

Fig. 1 Structure and power flow of stepped planetary gear stages (planet carrier not shown)

proportional to the tooth forces. In planetary gear systems, however, this relationship does not apply because of the multiple gear meshes. Depending on the phase of the individual mesh engagements, translational and rotational excitations can either superimpose or compensate each other. Due to this decoupling from the tooth forces, it is no longer sufficient in planetary gear systems to consider only one excitation component in isolation. According to Heider, translational excitation can be assessed either via bearing force excitation or through displacement behavior, while rotational excitation can be evaluated using either the torque level or the transmission error. [11]

While cylindrical gear systems typically exhibit excitations at the gear mesh frequency, planetary gearboxes are additionally affected by modulations. Inalpolat conducted a comprehensive parameter study involving various planetary gear configurations with a stationary ring gear to investigate the origin of these effects. The excitation behavior was measured using acceleration sensors mounted uniformly around the circumference of the ring gear. In all investigations, excitations were observed to occur symmetrically or asymmetrically around the tooth mesh order, at integer order distances. Inalpolat classified the examined planetary configurations with uniformly distributed planets into two categories: (i) systems with symmetric meshing sequence, and (ii) systems with sequential meshing sequence. The gearbox analyzed in this report, featuring double-sequential meshing and uniformly distributed stepped planets, belongs to the second category. Based on this classification, various characteristic influences on the excitation behavior were identified. According to Inalpolat, no excitation at the first tooth mesh order is observed in group (ii). Instead, asymmetric excitations arise at orders that are integer multiples of the number of planets. The highest amplitudes were found at the order closest to the tooth mesh order. Inalpolat attributed the observed modulation effects, the excitation occurring at integer orders away from the tooth mesh order to the characteristics of structure-borne noise measurement. The planet closest to a given sensor dominates the measurement excitation response. Due to its relative motion with respect to the sensor, it causes both amplitude and frequency modulation [12].

Theling also conducted test bench investigations on planetary gearboxes belonging to group (ii). The peak-to-peak transmission error between the sun and the carrier was used as the measurement quantity to characterize the excitation behavior. In the order spectrum, Theling observed the same modulation effects as previously described by Inalpolat [12]. As a result, the relative position of individual planets with respect to a structure-borne noise sensor can be excluded as the primary cause of the modulation. Theling attributed the modulation effects to positional deviations between the central elements of the system. These deviations lead to load imbalances that alternate between planets due to carrier rotation. On the one hand, a load imbalance results in amplitude modulation, where a single planet dominates the excitation. This leads to excitation at the mesh order itself rather than at integer multiples of the mesh order defined by the number of planets. In addition, frequency modulation occurs as the path of highest excitation shifts from one planet to another. In sequential meshing conditions, individual planets are phase-shifted. Consequently, each change in the dominant excitation path is accompanied by a phase jump. During one full carrier rotation, the number of phase jumps corresponds to the number of planets. Therefore, an order is always excited that is offset from the mesh order by a multiple of the planet-to-planet phase shift. [8]

The stepped planetary gear topology investigated in this paper exhibits a high degree of kinematic similarity to single-stage planetary gear systems. Consequently, similar excitation and displacement behavior can be expected. According to Inalpolat, characteristic modulated excitation patterns can be observed in various planetary gear configurations [12]. However, such modulation effects have not yet been identified in stepped planetary gear systems. Inalpolat attributes these modulation effects to the method of structure-borne noise measurement, whereas Theling explains them as a result of carrier axis misalignments [8, 12]. Investigations into carrier axis misalignments, combined with measurements of transmission error and structure-borne noise, may provide further insights in this context.

2.2 Displacements in stepped planetary gear stages

The operational behavior of a gearbox is ultimately determined by the contact conditions that occur under real operating conditions [13]. Deviations from an ideal gear mesh can be classified into translational and rotational displacements. In the case of stepped planetary gear systems, a further distinction must be made between misalignments of the stepped planets themselves and those of the central components. Additionally, in stepped planetary systems, such misalignments can lead to load imbalances during multiple meshing conditions. One approach to counteract this and to achieve load balancing is the use of elastic or floating components.

Deviations from the parallelism of the rotational axes of gears are referred to as rotational displacements. A deviation within the plane defined by the parallel rotational axes is described by Wittke as axis inclination, while a deviation in the perpendicular plane is referred to as axis skew [13]. Translational displacements include radial, axial, and tangential shifts of the gears relative to the central axis.

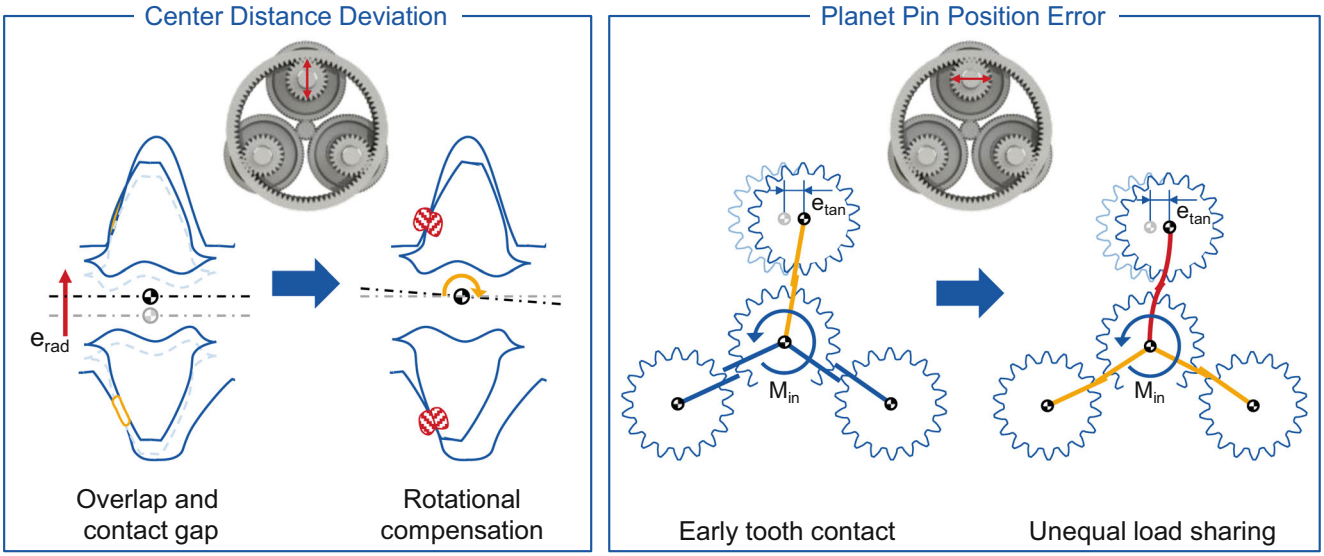

Fig. 2 Translational displacements according to [14, 15]

A radial displacement results in a change in center distance Δa.

The line of action in involute gear meshes corresponds to a straight line tangential to the base circles. This ensures that a change in center distance does not violate the fundamental law of gearing. However, a varying center distance changes the angle of the path of contact and thus the profile contact ratio, which in turn affects the total contact ratio. As a result, changes in center distance influence the overall mesh stiffness and thereby the parametric excitation [7]. A reduction in center distance also leads to a decreased backlash and may cause interferences of the gears [13].

In planetary gear systems, a change in the center distance at one central gear always leads to an opposite change at the other central gear. According to Iglesias et al., such a center distance variation causes a phase shift of the affected planet [14]. A reduced center distance causes the planet to engage earlier at one contact point, while increasing the backlash at the opposite contact. Due to force equilibrium, the planet rotates until contact is re-established at both meshes, see Fig. 2 left [14]. For a change in center distance to be fully compensated by a pure rotation of the planet, the pressure angles at both engagements must be identical. Otherwise, the resulting backlash is either too large or too small, leading to both a phase shift and an additional influence on load distribution [14]. A tangential displacement of the planet is also referred to as a planet pin position error. This causes the affected planet to engage earlier or later in both sun-planet and planet-ring contacts, depending on the direction of deviation, Fig. 2 right [14].

In the case of a planet pin position error, the planet that is ahead theoretically carries the entire load, or conversely, if one planet lags behind, the remaining planets are assumed to carry the full load instead [15]. Due to the applied torque, the corresponding teeth are already under load before the other planets come into contact, see Fig. 2 right. From that point onward, any additional load is distributed evenly across the available power paths. The force required to compensate for the misalignment leads to a significant deviation from the ideal load distribution. The lower the transmitted torque, the more uneven the load sharing becomes. As the torque increases, the proportion of force required for deformation decreases in relation to the total load [15].

3 Objective and approach

The operational behavior of planetary gear systems has already been the subject on numerous research studies. In contrast, only a few investigations exist regarding stepped planetary gear systems. In particular, there is currently a lack of sufficient experimental studies on the effects of axis misalignments on the excitation behavior. Building on the research of Westphal et al., this paper presents experimental investigations into the influence of axis misalignments in stepped planetary gear systems on excitation and displacement behavior [1].

According to the state of the art, rotational and translational axis misalignments in stepped planetary gear systems have differing effects on excitation and displacement behavior. Resulting load increases can be partially compensated by elastic or floating elements. In order to evaluate excitation behavior, both rotational and translational excitations must be considered in stepped planetary gear systems [11]. The literature discusses various explanations regarding the

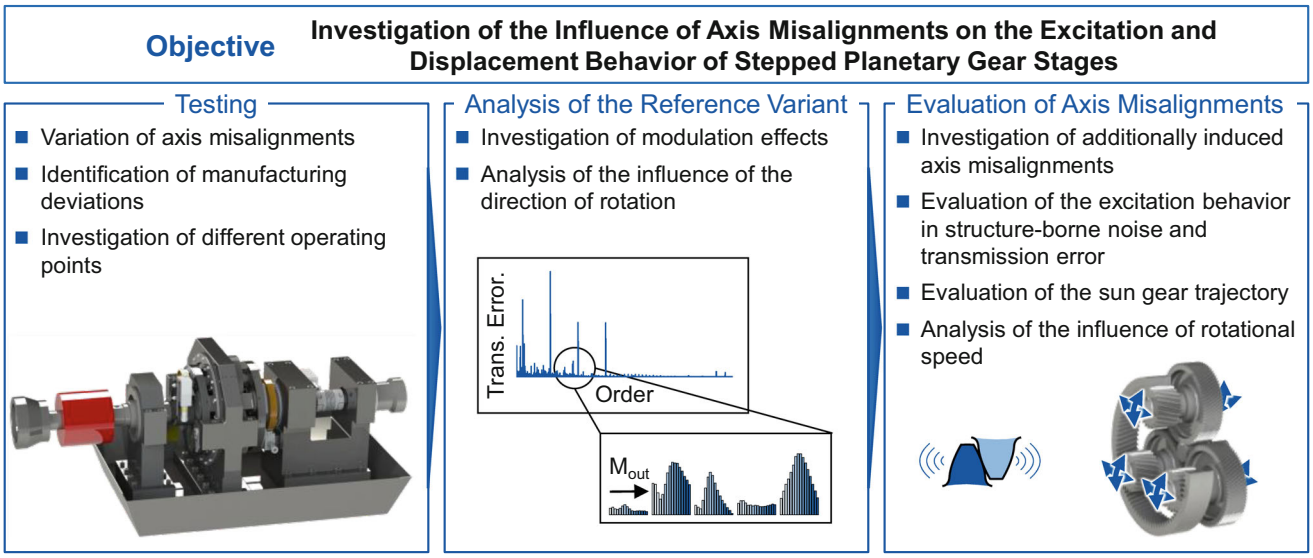

Fig. 3 Objective and approach

origin of modulation effects in planetary gear systems [8, 12].

Therefore, the objective of this paper is to investigate the excitation behavior based on transmission error and structure-borne noise, as well as to analyze the displacement behavior using the sun gear trajectory and carrier displacement, see Fig. 3. For the experimental investigations, a stepped planetary gearbox test rig is available at the WZL of RWTH Aachen University. By using eccentric bushings, specifically defined misalignment states can be applied to the otherwise rigid gearbox.

In the first step, the manufacturing and assembly deviations of the test rig are analyzed. Additionally, the test parameters and misalignment variants are defined. This is followed by experimental investigations in which measurement data are collected in the form of transmission error, structure-borne noise, and displacement behavior. Based on a reference configuration, modulation effects are analyzed, and characteristic orders are identified, serving as a foundation for further analysis. In a subsequent step, the influence of different axis misalignments of the stepped planets is systematically examined. The effects on transmission error, structure-borne noise, and displacement behavior are evaluated across various rotational speeds.

4 Experimental setup and test plan

The investigations into the excitation and displacement behavior of stepped planetary gearboxes were carried out using a test rig at the WZL. The test rig is based on a planetary gearbox test setup developed by Theling, which has already been used for similar studies on single-stage planetary gearboxes [8]. Westphal et al. adapted the test rig concept to a stepped planetary gearbox configuration and provided a detailed description of the setup [1, 10].

The gear manufacturing was carried out at the WZL. Due to the low production volume, power skiving was selected for the internal ring gear, while profile grinding was used for the external gears. For the geometrical characterization of the gears, full-tooth topography measurements were performed using the KLINGELNBERG P65 gear measurement center at WZL. All gears meet at least tolerance class 5 according to DIN ISO 1328-1 with regard to manufacturing accuracy [16]. In addition to the flank topography, pitch and runout deviations were also measured. The pitch deviation trends are shown on the left side of Fig. 4 for both the sun-planet 1 gear mesh and the planet 2-ring gear mesh. Furthermore, the phase offset between the two planets was determined via an alignment measurement. The specified teeth of the planets z_{P1} and z_{P2} were taken into account during the assembly of the stepped planets into the carrier and the phase alignment of the sun and ring gear during installation.

The positioning of the bearing blocks on the mounting plate as well as manufacturing deviations at the bearing locations determine the axis alignment of the central shafts. Likewise, the boreholes in the planet carrier plates have a significant influence on the alignment of the stepped planets. In order to ensure accurate alignment of the bearing blocks and to consider existing deviations in the analysis, components of the test rig were measured using a coordinate measuring machine from ZEISS (model: Zeiss Prismo Navigator). For each bearing location, measurement circles were recorded, and a reference coordinate system was de-

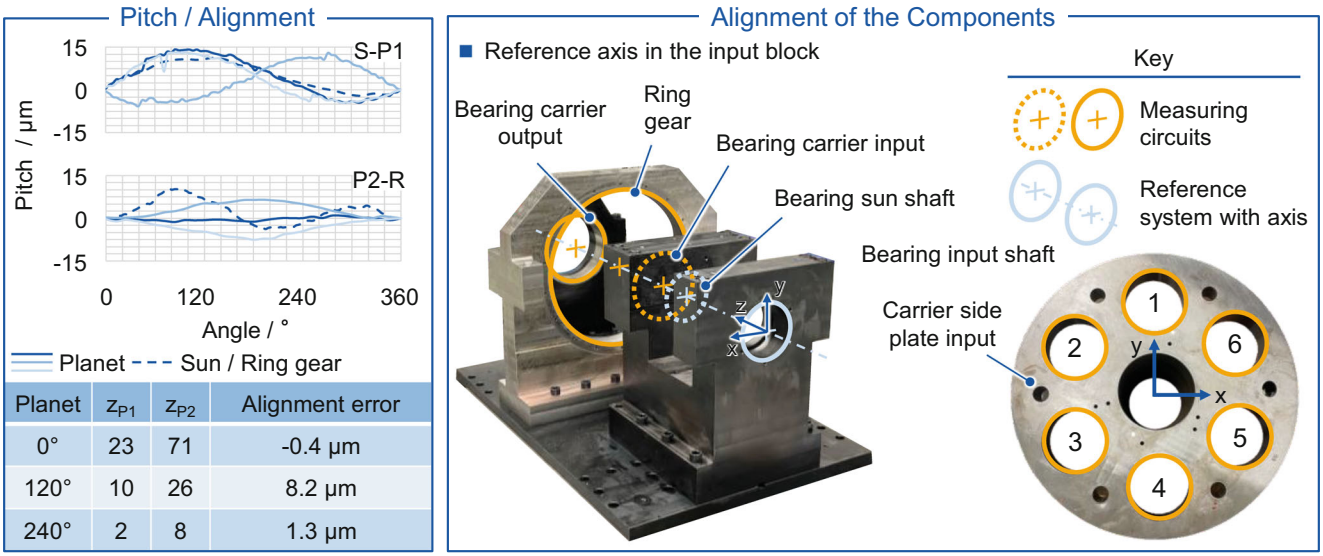

Planet	z_{P1}	z_{P2}	Alignment error
0°	23	71	-0.4 µm
120°	10	26	8.2 µm
240°	2	8	1.3 µm

Fig. 4 Measurement of manufacturing quality and assembly deviations

fined at the input shaft bearing, aligned with the sun shaft bearing, see Fig. 4 right.

Based on the center points determined from the measurement circles, translational deviations of the carrier and ring gear mounting positions were identified relative to the reference coordinate system. The bearing blocks are not pinned to the mounting plate, which means they must be manually aligned during assembly. The actual positional deviations in the fully assembled state are listed in Table 1. A notable aspect is the predominantly vertical offset in the y-direction between the carrier bearing position and the ring gear. This misalignment results from manufacturing deviations and cannot be corrected during assembly. Compensation using eccentric bushings is not possible in this case, as the reference configuration already utilizes the maximum upward eccentric offset at the carrier bearings. Carrier misalignments result in varying mesh conditions for the planets around the circumference. For example, depending on the angular position of a stepped planet, a vertical offset of the carrier can temporarily increase or decrease the center distance, or lead to a positive or negative planet pin position error. These effects are sinusoidally distributed and phase-shifted by one quarter of a carrier revolution [8].

In addition to the determined position of the carrier, the carrier side plates were also geometrically characterized, see Fig. 4 bottom right. The carrier plates contain six equally spaced bores of identical dimensions, which are used either for mounting the planets or for connecting struts. To identify suitable bores for the stepped planets, the position of the bores on both carrier plates were analyzed. For this purpose, measurement circles were used, and the center point displacement was converted into an axis offset and a planet pin position error. The results of this measurement are shown in Table 2. A positive planet pin position error corresponds to a mathematically positive rotation around the z-axis.

All position deviations are within the specified manufacturing tolerances. However, the deviations at the input-side carrier plate are up to four times higher than those at the output-side plate. On the input-side carrier plate, bores one, three and five were selected to ensure the lowest possible pitch error between the stepped planets. On the output-side carrier plate, the deviations are nearly identical across all bores. For simplification, bores one, three and five were also selected on this side, as existing bores for sensor mounts were already available at these positions. In the following, the stepped planet position in bore one is referred to as 0°, in bore three as 120°, and in bore five as 240°.

The investigations are carried out at various constant input torques and a constant rotational speed in order to elim-

Table 1 Misalignments of the components

Deviation	Bearing carrier input	Ring gear	Bearing carrier output
Δx / μm	11.4	–9.0	–7.3
Δy / μm	–10.9	–19.3	–43.3
Δz/ μm	–159.1	–97.4	–32.9
$\Delta\varphi_x$ / °	–0.023	–0.012	0.014
$\Delta\varphi_y$ / °	0.006	–0.013	0.010

Table 2 Geometric deviations in the planet carrier side plates

Input-side carrier plate			Output-side carrier plate		
Bore	Center dist. deviation / µm	Planet pin pos. error / μm	Bore	Center dist. deviation / μm	Planet pin pos. error / μm
1	*10.57*	*0.77*	*1*	*1.36*	*–0.48*
2	–3.43	–6.43	2	–2.61	–1.09
3	*–13.58*	*7.25*	*3*	*–1.48*	*–0.50*
4	–9.48	19.42	4	–4.68	–2.57
5	*1.60*	*23.28*	*5*	*–2.26*	*–5.15*
6	12.48	16.40	6	1.16	–4.11

Table 3 Axis misalignments of the stepped planets

Variant	Combined axis misalignment of the first stage Combined axis misalignment of the second stage			
	Center distance deviation P0° | P120/240°	Planet pin position error P0° | P120/240°	Inclination P0° | P120/240°	Skew P0° | P120/240°
Reference	0 µm | 0 µm	0 µm | 0 µm	0 µm | 0 µm	0 µm | 0 µm
	0 µm | 0 μm	0 µm | 0 μm	0 µm | 0 μm	0 µm | 0 μm
Skew	*71 μm | 100 μm*	*25 μm | 0 μm*	0 µm | 0 μm	*–23 μm | 0 μm*
	71 μm | 100 μm	*–22 μm | 0 μm*	0 µm | 0 μm	*–33 μm | 0 μm*
Inclination	*–25 μm | 71 μm*	0 µm | 0 μm	*23 μm | 0 μm*	0 µm | 0 μm
	22 μm | 71 μm	0 µm | 0 μm	*33 μm | 0 μm*	0 µm | 0 μm
Pos. planet pin pos. error	*87 μm | 87 μm*	*100 μm | 0 μm*	0 µm | 0 μm	0 µm | 0 μm
	87 μm | 87 μm	*100 μm | 0 μm*	0 µm | 0 μm	0 µm | 0 μm
Neg. planet pin pos. error	*87 μm | 87 μm*	*–100 μm | 0 μm*	0 µm | 0 μm	0 µm | 0 μm
	87 μm | 87 μm	*–100 μm | 0 μm*	0 µm | 0 μm	0 µm | 0 μm

inate dynamic influences caused by changes in speed or torque. The torque levels for the tests are determined based on the motor characteristics and the component with the lowest transferable torque. The metal bellows coupling is rated for a torque of $M_{max} = 150$ Nm, which is therefore defined as the upper limit for the input torque Min. The maximum speed is limited by the slip ring transmitter on the output side to $n_{out, max} = 200$ rpm, corresponding to $n_{in, max} = 3328.2$ rpm. For the quasi-static investigations, two opposing requirements must be considered. On the one hand, a high rotational speed is desirable in order to achieve a high number of carrier revolutions within the defined measurement time of $t = 60$ s to allow for the identification of low-frequency excitation components. On the other hand, a low and resonance-free speed is required to minimize the influence of dynamic effects. Based on a dynamic run-up from $n_{in} = 400$ rpm to $n_{in} = 2000$ rpm at a constant torque of $M_{out} = 385.5$ Nm, natural frequencies of the test rig were identified. Figure 5 left shows the frequency-based Campbell diagram of this test. At a frequency of approximately $f \approx 1200$ Hz, a natural frequency appears, which correlates with a simulated natural frequency of the ring gear mounting block. The second harmonics of the gear mesh frequency of the first stage $O_{z, S\text{-}P1}$ enters the range of this natural frequency at approximately $n_{in} \approx 1400$ rpm. Based on this analysis, a maximum input speed of $n_{in} = 1000$ rpm was defined to ensure that no resonance-induced amplification of the excitation occurs. To verify whether dynamic effects arise at the selected test speed, additional trial measurements were conducted at a reduced input speed of $n_{in} = 500$ rpm.

As described by Westphal et al., a misalignment of the corresponding shaft can be induced by rotation of the eccentric bushings at the bearing locations of both the stepped planet shafts and the planet carrier [1]. The bushings exhibit an eccentricity of $e = 100\,\mu$m between the inner and outer cylindrical surfaces. The bearing span amounts to $L_{G, Planet} = 215$ mm for the stepped planets and $L_{G, Carrier} = 511$ mm for the carrier. If the rotation of two opposing eccentric bushings occurs in the same direction, a translational displacement of the respective shaft results, see Fig. 5 top right. In contrast, counter rotation of the bushings leads to a rotational displacement, see Fig. 5 bottom right. The reference configuration is defined by aligning all planet eccentric bushings tangentially in the same direction relative to the carrier. Based on this configuration, four planet misalignment variants are investigated, as listed in Table 3. The values presented in Table 3 describe the resulting displacement state of the gears in the first and second stage. The variants are labeled based on the displacement component that defines the respective case. To

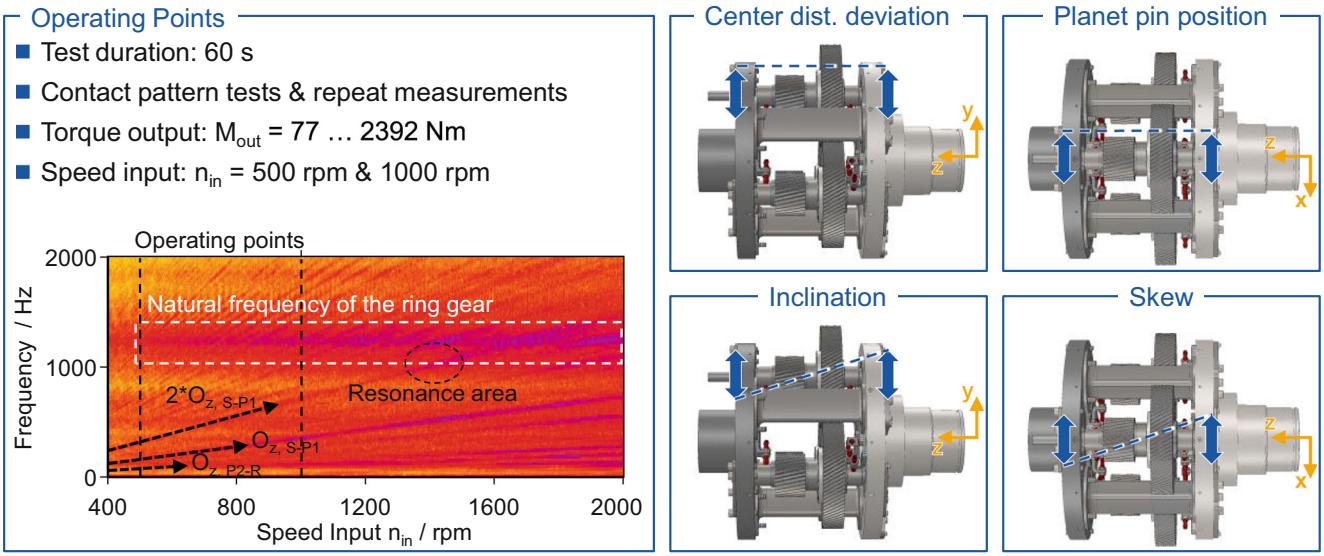

Fig. 5 Operating point and variation of axis misalignments

provide additional context, the inclination and skew components can be transformed into a lead angle deviation of the tooth contact [13]. For the skew variant, this results in an absolute lead angle deviation of Planet 0° with $F_{H\beta,\,P0,Skew,\,Stage\_1} = 21.2\,\mu m$ and $F_{H\beta,\,P0,Skew,\,Stage\_2} = 31.2\,\mu m$, and for the inclination variant with $F_{H\beta,\,P0,Inclination,\,Stage\_1} = 9.0\,\mu m$ and $F_{H\beta,\,P0,Inclination,\,Stage\_2} = 10.4\,\mu m$. In principle, the misalignments applied to a single stepped planet (Planet 0°) are investigated. Due to the circular motion of the eccentric bushings, combined misalignments may occur. Therefore, the remaining stepped planets (Planet 120° and Planet 240°) are positioned in such a way that pin position errors arising from rotatory misalignments are partially compensated, and center distance changes are as uniform as possible across all planets.

All tests are conducted in the mathematically negative direction of rotation, meaning that the left tooth flanks of the planet gears are in contact. This configuration is referred to as counterclockwise rotation in this paper. A positive planet pin position error indicates that the test planet is shifted along the circumference in the positive direction of rotation. In counterclockwise rotation, this results in a shift into the gear mesh and a load increase on the corresponding planet gear. For all tests, the input torque is applied via the sun gear. Prior to each test series, the test rig is brought to a steady-state operating temperature by means of a warm-up run lasting $t_{warm\text{-}up} = 40\,min$, with an output torque of $M_{out,\,warm\text{-}up} = 1312\,Nm$ and an input speed of $n_{in} = 500\,rpm$. During operation, a volume flow of $\dot{V}_{Oil} = 60\,ml/s$ of Shell Spirax MA 80 W oil is supplied to the test rig at an oil temperature of $t_{oil} = 60\,°C$.

5 Analysis of the excitation and displacement behavior

This chapter evaluates the measurement results regarding the excitation and displacement behavior of stepped planetary gear stages. The reference variant is initially described in detail, with relevant excitation frequencies identified for further analysis. Subsequently, different types of axis misalignments as well as various rotational speeds are analyzed.

5.1 Investigation of the excitation behavior of the reference variant

To assess the influence of different axis misalignments on the excitation and displacement behavior, the reference variant is first examined in detail. It should be noted that the reference already exhibits deviations from the ideal axis alignment due to manufacturing errors. Noteworthy are, on the one hand, the planet pin position error resulting from misalignments of the boreholes in the input-carrier plate, see Table 2. On the other hand, manufacturing deviations at the carrier bearing locations lead to axis misalignments of the central shafts, see Table 1.

The excitation behavior is evaluated based on the total transmission error between the sun gear and the carrier, the single-stage transmission error between the sun gear and the measuring planet, as well as the structure-borne noise. From the encoder signals, the rotation angle differences are determined considering the respective gear ratio. Using the center distance $a = 112.5\,mm$, the transmission error is calculated. A Fast Fourier Transform (FFT) is then applied to decompose the resulting time signal into its excitation

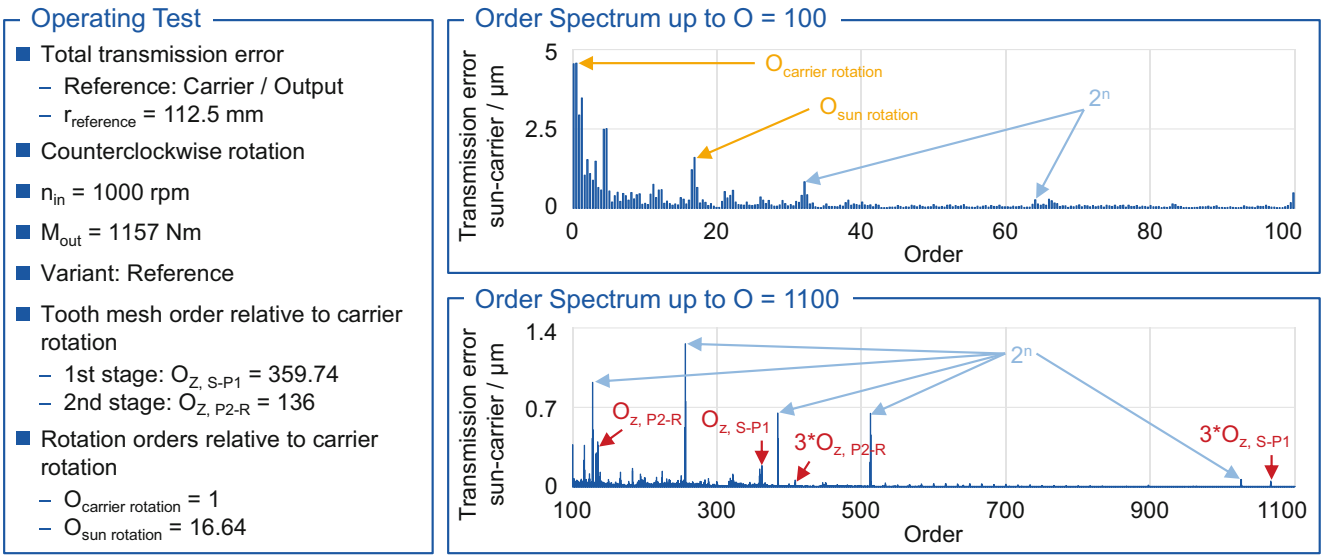

Fig. 6 Order spectrum of the reference variant

components, enabling the identification and comparison of excitation sources [7]. In a stepped planetary gear stage, a wide range of frequencies can be excited. These include the short-wavelength meshing frequencies of the individual gear stages, as well as long-wavelength excitations related to the rotational and hunting tooth frequencies of the sun gear, planet gears, and the carrier. Additionally, there are excitations that do not originate directly from the gearbox, but rather from the surrounding test bench setup. These include, for example, the bearings, intermediate gearbox, both electric motors, and the measurement system. Furthermore, higher-order harmonics of the respective excitation frequencies occur. To identify interference frequencies from the test bench environment, the signals are compared with the measurements of the acceleration sensors mounted on the respective bearing blocks.

Figure 6 shows the order spectrum of the total transmission error at a medium torque level of $M_{out} = 1157\,Nm$. The spectrum is depicted for orders up to $O = 100$ at the top and for the higher orders up to $O = 1100$ at the bottom. The lower order range shows high amplitudes of the transmission error. Notably, the excitation in the carrier rotational order is several times higher than that of the surrounding orders. Amplitudes at orders that are integer multiples of 2^n result from the measurement system and are not further discussed. According to Neubauer, planetary gear stages with three planets and sequential meshing exhibit maximum excitation amplitude from the tooth contact at the third tooth mesh order [17]. However, the present spectrum shows excitation at the first tooth mesh order $O_{z,i}$ for both the first and the second stage, see Fig. 6 bottom. This suggests that one of the planets transmits more load, undergoes greater deformation, and consequently dominates the excitation behavior. This may be caused either by axis misalignments due to deviations at the carrier bearing locations. Since the floating sun gear is expected to enable a static load balancing under constant deviations, this observation tends to indicate the presence of amplitude modulation, as described by Theling [8]. For this reason, the order region around the two tooth mesh orders is analyzed in more detail in the following.

According to Theling, axis misalignments of the central gears in planetary gear systems with sequential meshing lead not only to amplitude modulations, but also frequency modulations [8]. The frequency modulation depends on the phase shift present at the central gears. In the investigated gearbox, different phase shifts of the individual planets are present in each stage. In the first stage, the planet at $\varphi_{carrier,\,P120°} = 120°$ has a phase shift of $\Delta p_{sun,\,P120°} = 2/3$, and in the second stage of $\Delta p_{ring\,gear,\,P120°} = 1/3$. For the other planet P240°, the relationship is reversed, with $\Delta p_{sun,\,P240°} = 1/3$ und $\Delta p_{ring\,gear,\,P240°} = 2/3$. If an increased load share occurs due to axis misalignments of the central elements, it always arises at the same location of the stationary ring gear. Due to the carrier rotation, however, the planet experiencing the maximum load continuously changes. Consequently, the sequence in which the planets are subject to this overload also depends on the direction of rotation. In the case of counterclockwise rotation, following the first planet, P120° and subsequently P240° pass the same location. Top center in Fig. 7 illustrates the origin of the frequency shift during counterclockwise rotation for the first stage. The stepped planet carrying the highest load determines the excited order through amplitude modulation. When the path of maximum load changes, an additional phase shift in excitation occurs, depending on the existing phase shift. The resulting

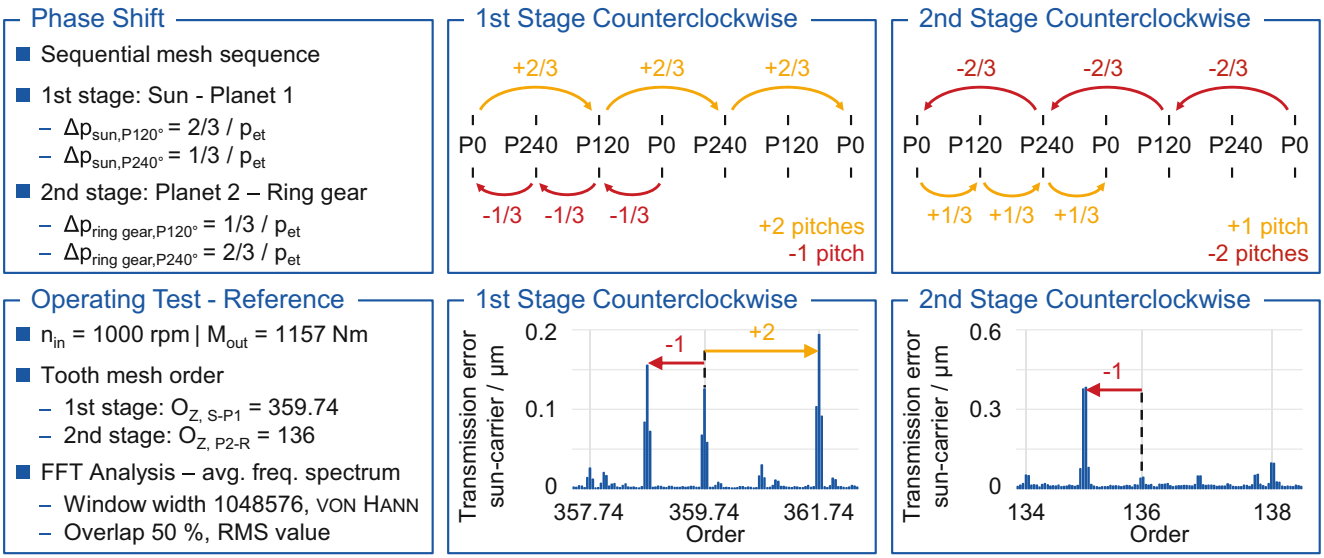

Fig. 7 Frequency modulations

excitation may lead by two-thirds of a base pitch or lag by one-third. With three planets, this process repeats three times per carrier rotation, as the path of maximum excitation changes three times. As a result, an excitation occurs that lies either two pitches above or one pitch below the original mesh order. Due to the different phase shift in the second stage, a similar mechanism results in an expected excitation that lies one pitch above or two pitches below the mesh order, see Fig. 7 top right.

The transmission error of the reference variant in counterclockwise rotation is shown in the order ranges of both mesh orders in the lower section of Fig. 7. In both gear stages, frequency modulations occur at orders deviating by one or two integer multiples of the pitch from the respective mesh order. This confirms modulation effects that were previously observed in planetary gear systems by Theling and can now also be identified in stepped planetary gear stages [8]. In the first stage, the excited orders correspond to those predicted by theoretical considerations, see central section of Fig. 7. In contrast, the second stage exhibits deviations from the expected excitation patterns, as shown on the right side of Fig. 7. Moreover, it is noticeable that in the second stage, a single order stands out with a significantly higher amplitude than the others. This dominant order trails the mesh order by one pitch, is divisible by the number of planets, and lies closest to the original mesh order. Such behavior aligns with the predictions of Inalpolat, who observed similar excitation patters in single-stage planetary gearboxes with sequential meshing [12]. In comparison, the sun-planet stage shows several orders excited with similar amplitudes, see central lower part of Fig. 7. This behavior may be attributed to the floating sun gear, which leads to variable contact conditions. The influence of this floating behavior may also be reflected in the excitation of the original mesh order. Notably, this order is only significantly excited in the stage where the sun gear actively compensates for load imbalances.

The investigations reveal that, in addition to the tooth mesh frequencies, modulated frequencies are also excited. It appears that, despite the use of a floating sun gear, load imbalances may still occur that cannot be fully compensated. The location of the excited frequencies can only partially be explained using the approach proposed by Theling [8]. One possible reason for this discrepancy is that, due to the additional mesh frequencies in a stepped planetary gearbox, further interactions may arise. In addition, it is assumed that load imbalances caused by carrier misalignments occur at a specific location and are sequentially passed by the planets once per carrier revolution. This assumption may not hold true, and the test bench might exhibit a more complex behavior in which the path of maximum excitation varies. Additionally, an influence of the floating sun gear was identified. The compensating motion of the sun gear, resulting from its one-sided bearing support, also induces a rotational axis misalignment. This may lead to altered meshing conditions, causing a time-varying phase shift. In his test bench investigations, Theling did not include a floating sun configuration, limiting the possibility of load compensation to elastic mechanisms only [8]. Therefore, in further investigations of the influence of axis misalignments on excitation behavior, it is essential to analyze not only the primary tooth mesh order but also the adjacent orders at $\Delta O = \pm 1$ and $\Delta O = \pm 2$ pitches.

5.2 Influence of axis misalignments of the stepped planet

The influence of axis misalignments on the operational behavior is analyzed based on induced axis misalignments of the planet shafts. A defined displacement is introduced into the system by rotating eccentric bushings at the bearing locations in the planet carrier. In each case, the measuring planet P0° is misaligned relative to the other two planets. The test plan includes the reference case, an inclination, a skew and both a positive and a negative planet pin position error, see Table 3. Due to the rotation of the eccentric bushings, all variants exhibit not only the intended displacement but also a combined axis misalignment.

5.2.1 Evaluation of the excitation behavior

Figure 8 shows the excitation in the first stage based on the overall transmission error. As explained in the previous chapter, not only the tooth mesh order $O_{Z,\,S\text{-}P1}$, see Fig. 8 bottom left, but also the surrounding orders at $\Delta O = \pm 1$ and $\Delta O = \pm 2$ pitches are considered. Already in the reference case, it was observed that more frequencies are excited in the first stage than in the second. For the misalignment variants inclination and planet pin position errors, the order at $\Delta O = +1$ pitch is additionally excited to a significant extent, see Fig. 8 bottom center. These misalignments lead to a load imbalance that must be compensated by sun gear movement. The fact that an additional frequency is excited when further misalignments are applied supports the assumption that the sun gear movement influences the frequency modulation in the order range of the stage in which the sun-planet contact occurs. It is also noticeable that the inclination variant shows an almost identical response to the reference across all orders, see Fig. 8. This is consistent with findings by, for example, Iglesias et al. who observed that rotational misalignments have up to 40 times less influence on load distribution behavior compared to planet pin position errors [14]. The inclination variant is the only configuration without a combined planet pin position error component, which explains the comparatively low excitation. The tangential deviation induced by the eccentric bushings is, at $e_{eff} = 100\,\mu m$, larger than the planet pin position error that results from the vertical offset carrier at certain angular positions of the carrier, caused by manufacturing deviations. As a result, the measurement planet affected by the imposed planet pin position error is located furthest ahead or behind on the circumference, regardless of the position of the other planets. This implies that the maximum excitation no longer varies, or varies significantly less, with the carrier rotation, and the resulting frequency modulation effects no longer occur. In theory, during counterclockwise rotation in the first stage, the orders excited are not the tooth mesh order itself, but those at $\Delta O = -1$ pitch and $\Delta O = +2$ pitches, see Fig. 7. However, it is precisely at these frequencies that the planet pin position errors result in the lowest excitation, see Fig. 8 right. In contrast, the planet pin position errors lead to the highest excitation in the tooth mesh order, see Fig. 8 bottom left. Consequently, for the misalignment cases where no frequency modulation due to a shift in the path of maximum excitation is expected, an opposite trend is observed. This result supports the theory of modulation formation in planetary gearboxes as proposed by Theling [8].

The fact that this behavior is more pronounced for the negative pin position error than for the positive one is also consistent. In the counterclockwise rotation, the manufacturing deviation of the position of the boreholes on the input-side carrier plate already results in an effective negative pin position error for the measuring planet compared to the other planets, see Table 2. As a result, the axis misalignment induced by the eccentric bushings is higher negative in the case of a negative pin position error and less positive in the case of a positive one. Consequently, the path of highest excitation is less affected by the carrier misalignment when a negative pin position error is present than when a positive one is applied.

For comparison, Fig. 9 shows the influence of rotational speed on the excitation behavior based on the overall transmission error at the top and the structure-borne noise measured at the ring gear in the vertical direction at the bottom. The evaluation focuses on both the tooth mesh order and the order increased by $\Delta O = +2$ pitches in the first stage. As examples, the two types of rotational axis misalignments, skew and inclination, as well as the negative planet pin position error are considered. At the rotational speed of $n_{in} = 1000\,rpm$ a comparable trend between the structure-borne noise and the transmission error can be observed in both orders. Only the initial decrease in the transmission error in the tooth mesh order up to a torque of $M_{out} = 540\,Nm$ cannot be seen in the structure-borne noise signal, see Fig. 9 center. Therefore, the influence of the type of measurement, previously cited by Inalpolat as a potential cause for these modulation effects, can be ruled out [12].

For the investigations at a reduced speed of $n_{in} = 500\,rpm$, trial measurements were carried out at four torque levels. The excitation characteristics are identical for both speed variants. In the tooth mesh order, both the overall transmission error and the structure-borne noise are approximately twice as high for the negative planet pin position error compared to the rotational axis misalignments, see Fig. 9 center. In the order $O_{Z,\,S\text{-}P1,\,+2} = 361.74$, the behavior is reversed, with higher excitation for the rotatory misalignments, see Fig. 9 right. Notably, the transmission error in the mesh order is significantly higher at the lower rotational speed for both the skew and the negative pin position error com-

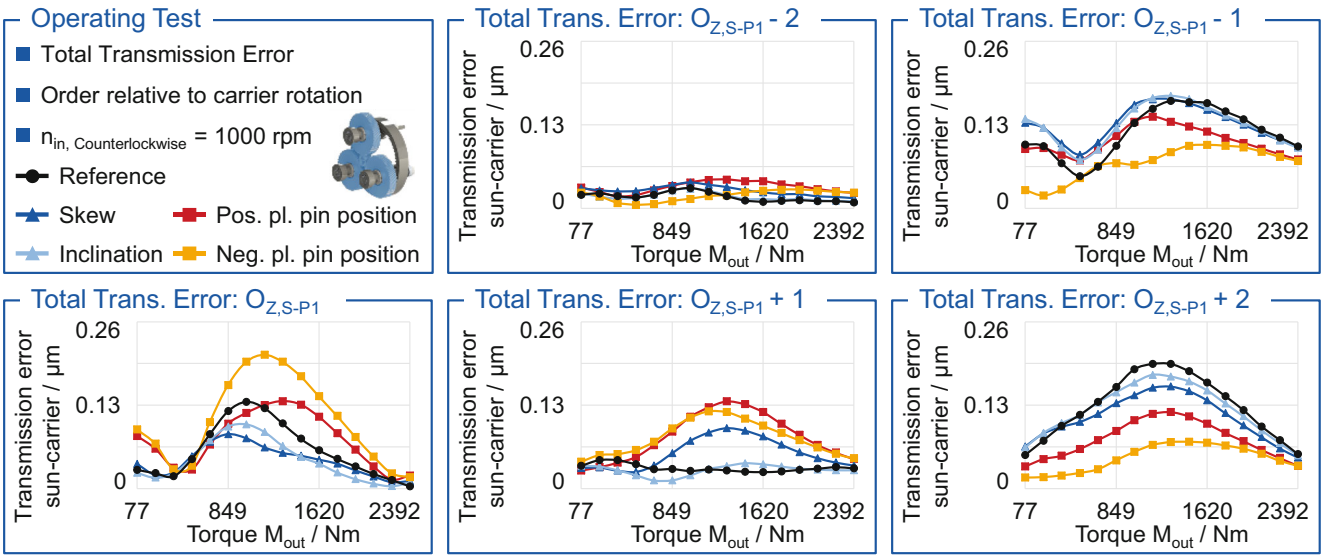

Fig. 8 Excitation in the tooth mesh order of the first gear stage

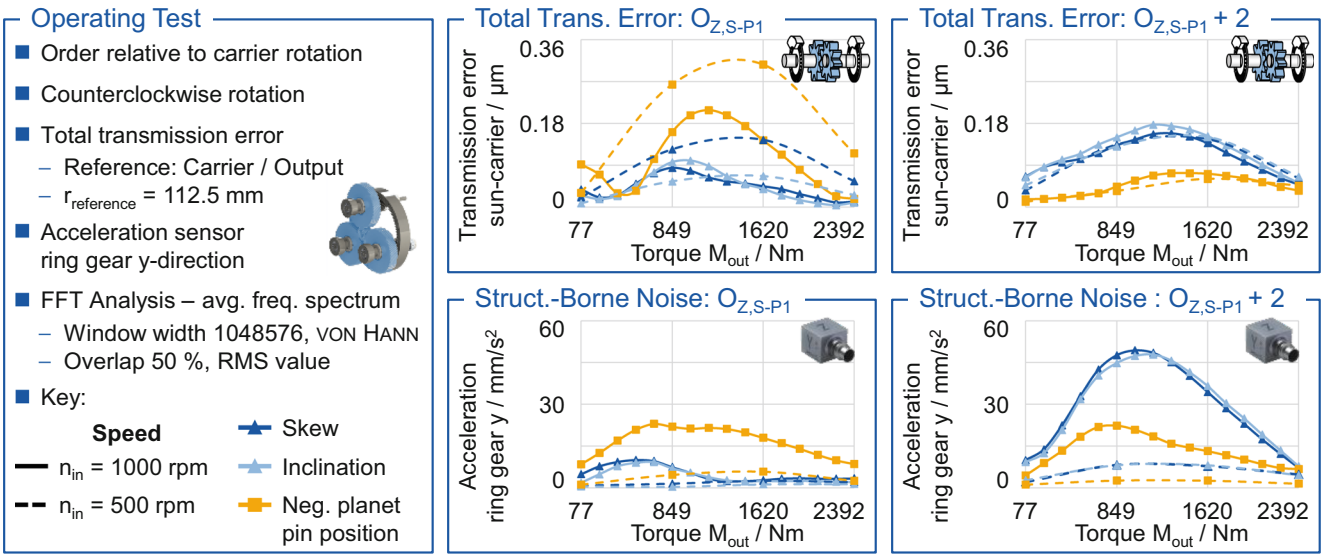

Fig. 9 Influence of rotational speeds on transmission error and structure-borne noise

pared to the reference speed of $n_{in} = 1000$ rpm. In contrast, the excitation in the modulated frequency remains independent of rotational speed. A resonance-induced amplification can therefore be ruled out, as this would also affect adjacent orders. However, the structure-borne noise excitation is significantly lower at $n_{in} = 500$ rpm than at $n_{in} = 1000$ rpm for both considered orders.

Figure 10 illustrates the excitation behavior of the first carrier rotation order $O_{C,1}$ in the center and the third carrier rotation order $O_{C,3}$ right. The upper diagrams show the overall transmission error between the sun and the carrier, while the lower diagrams display the structure-borne noise measured in the vertical direction on the ring gear. In contrast to the excitation observed in the mesh orders, the transmission error and structure-borne noise signals exhibit different behaviors in this case. The presence of a signal in the transmission error that is not observed in the structure-borne noise may be attributed to the effects within the transfer path, see Fig. 10 center. On the other hand, the excitation in the third carrier rotation order observed in the structure-borne noise suggests a potential correlation within the number of planets. The localized proximity of the planets to the acceleration sensor on the ring gear may lead to increased excitation in the structure-borne noise. These observations support the considerations of Heider, who emphasized that both the translational and rotational

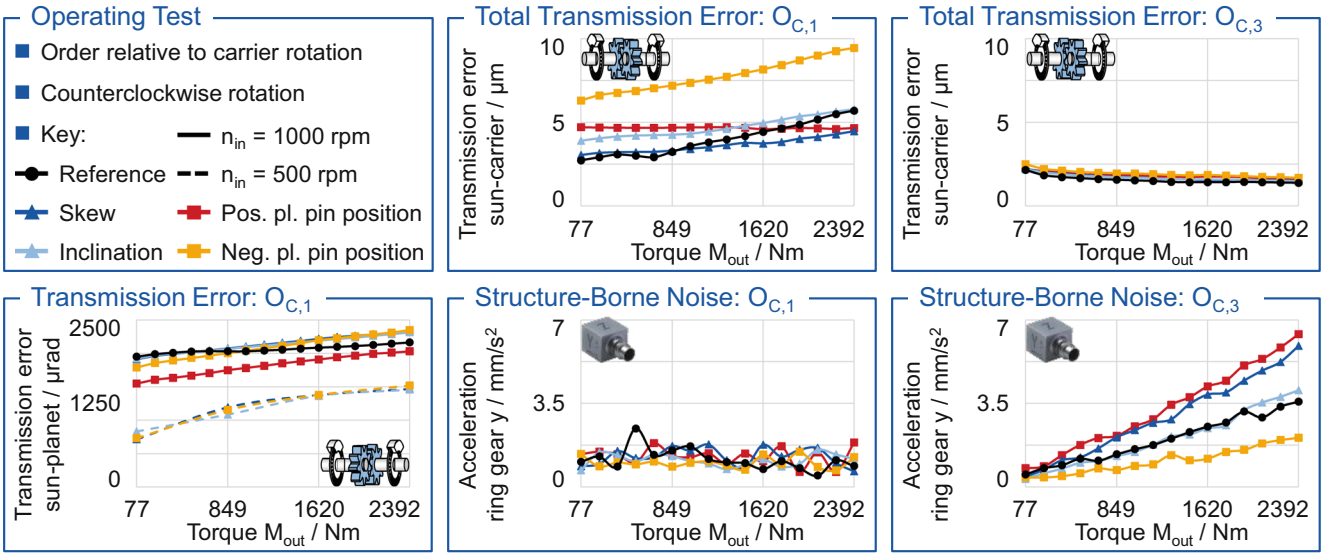

Fig. 10 Excitation in the carrier rotational order

excitations must be taken into account when evaluating the excitation behavior of planetary gearboxes [11].

In the overall transmission error within the first carrier rotation order, an influence of the misalignments on the excitation can be observed, see Fig. 10 center. In particular, the variant with a negative planet pin position error deviates noticeably from the others. At the lowest torque level, the transmission error is more than twice as high compared to the reference. Apart from the positive planet pin position error, the excitation increases with rising torque for all other variants. The rotational misalignment variants and the reference exhibit largely similar behavior. Since only the planet pin position errors differ, this indicates the influence of a load imbalance. It is possible that the sun gear is unable to fully compensate for the load imbalance occurring in the case of the negative pin position error. This imbalance then leads to increased excitation per carrier revolution. This finding is consistent with the simulation results of Westphal et al., which show that load imbalances can occur despite a floating sun gear when planet pin positions error are present [1]. In the structure-borne noise signal within the third carrier rotational order, an inverse sequence of excitations among the different variants can be observed, see Fig. 10 bottom right. The excitation from the negative planet pin position error is significantly lower than for the other variants. As the amount of positive pin position error in the misalignment increases, so does the excitation. For the reference and the inclination variant, only a small pin position error is introduced by the borehole position deviations in the carrier side plates. In the case of skew, the eccentric bushings cause a combined axis misalignment with a pin position error component. The highest excitation is observed for the positive pin position error. Figure 10 bottom left shows the single mesh transmission error between the sun gear and the planet. In contrast to the overall transmission error, no clear dependence on the misalignment conditions can be seen here. The excitation in this order could be attributed to the axis offset of the planet carrier. Due to this offset, the planet must perform a rotational compensation once per carrier revolution. The resulting excitation is proportional to the rotational speed and independent of the misalignment condition of the planets. This result suggests that the variation in excitation in the carrier rotation order originates from the ring gear contact but cannot be identified in the structure-borne noise signal.

5.2.2 Evaluation of the sun gear trajectory

For analyzing the displacement behavior of the stepped planetary gear stage, the sun gear trajectory is of relevance. To evaluate the influence of planet axis misalignments on the displacement of the sun gear, the resulting sun gear trajectories are shown in Fig. 11 for the highest torque level of $M_{out} = 2392\,Nm$ at $n_{in} = 1000\,rpm$ and $n_{in} = 500\,rpm$. For improved clarity, the axes for the pin position error cases shown at Fig. 11 bottom are scaled by a factor of 1:2 compared to the reference and the rotatory misalignment variants shown at the top. Planet pin position errors exhibit a significantly greater influence on the trajectory than the other variants. For both positive and negative pin position errors, the inner and outer radii are enlarged, whereas rotatory axis misalignments do not significantly alter the trajectory compared to the reference.

Figure 11 shows the influence of rotational speed on the displacement behavior for a negative pin position error at

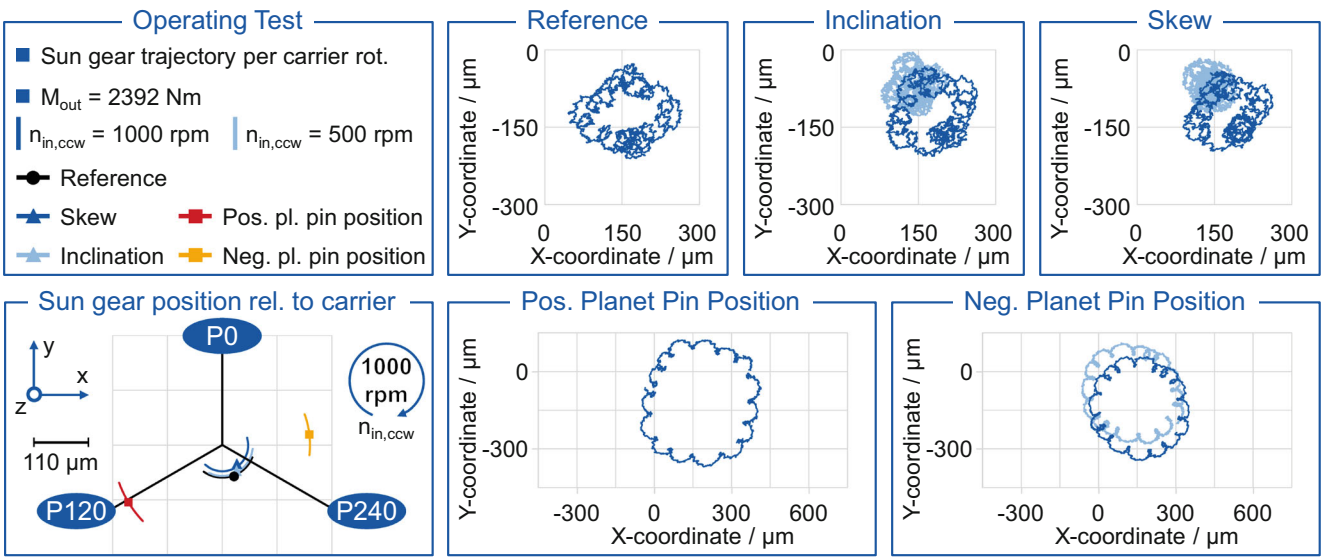

Fig. 11 Sun gear trajectory under axis misalignments

the bottom right and for rotatory axis misalignments in the center and top right. In all three cases, the center displacement of the sun gear trajectory at $n_{in} = 500$ rpm is approximately 25% lower compared to that at $n_{in} = 1000$ rpm. The loop-shaped displacement superimposed on the circular trajectory is similarly pronounced for all variants as well. Especially in the planet pin position error variants the loops are clearly visible. Since neither the type of misalignment nor the rotational speed affects the magnitude of the loops, this suggests a geometric deviation of the sun gear. Per carrier revolution, $n_{loops} = 15.6$ loops occur, corresponding to the number of relative sun gear rotations with respect to the carrier. The loops can therefore likely be attributed to a pitch deviation of the sun gear. In contrast, the effect of rotation speed on the radial expansion of the sun gear differs. For the cases with rotational axis misalignments, the radial expansion of the sun gear trajectory is significantly reduced at lower speeds, whereas it remains constant in the case of a negative planet pin position error. This suggests that constraint forces in the case of the pin position error hinder the expansion caused by inertial forces.

Based on Fig. 11 bottom left, the angular position of the sun gear relative to the carrier is analyzed for the torque level of $M_{out} = 2392$ Nm at $n_{in} = 1000$ rpm. The polar coordinate plot illustrates the angular position of the sun relative to the carrier and to the planets P0°, P120° and P240°. Each arc represents the range between the minimum and maximum angular deflection of the sun with respect to the carrier. The radial distance from the center of the plot corresponds to the average radius of the sun gear trajectory. The analysis first focuses on the positive planet pin position error of planet P0°. For the counterclockwise rotation shown here, this axis misalignment means that the test planet is shifted along the circumference in the negative x-direction into the mesh contact. As a result, this planet initially carries the full load, and the sun gear is deflected by the resulting forces. If only the contact forces from planet P0° act on the sun gear, the displacement is directed towards planet P120°, due to the vector sum of the tangential and radial contact forces. As the sun gear displaces, the other two planets also come into contact, establishing a load sharing condition. In contrast, a negative planet pin position error causes the test planet to be shifted out of the mesh. The resulting sun gear motion is now driven by the superimposed contact forces of Planet P120° and P240°. Although the sun gear is significantly displaced from its center position in both cases, the angular variation of the sun relative to the carrier during one carrier revolution remains limited with $\Delta\varphi_{Sun,\,pos.\,pin\,position} = 23.5°$ and $\Delta\varphi_{Sun,\,neg.\,pin\,position} = 27.1°$ respectively. In contrast, the radial displacement of the sun gear is smaller for the rotary axis misalignments and the reference configuration. Previous analyses in this chapter have already indicated that the variants with planet pin position errors are less affected by load imbalances resulting from carrier misalignments. This is due to the large imposed tangential deviation, which primarily determines the path of the highest excitation. For other variants, however, modulation effects were observed that can be attributed to a shift in the path of maximum excitation. This shift is also reflected in the angular position of the sun gear. A local load increase on one planet causes the sun gear to be displaced more strongly by the corresponding reaction forces. As the planet carrying the highest load changes circumferentially, varying force conditions occur. This leads to a broader range of angular displacement of the sun relative to the carrier, with values of $\Delta\varphi_{Sun,\,reference} =$

103.15°, $\Delta\varphi_{\text{Sun, inclination}} = 108.8°$, and $\Delta\varphi_{\text{Sun, skew}} = 148.1°$, respectively.

The effect of stepped planet axis misalignments is consistently superimposed by the manufacturing induced misalignment of the carrier. As a result, it is difficult to assign a clear influence on the excitation behavior to individual misalignment types. Modulation effects occur in both the transmission error and the structure-borne noise, and the influence of planet pin position errors on the modulation behavior can be explained based on the approach proposed by Theling [8]. The sun gear trajectory is affected differently depending on the type of planet axis misalignment. Even at relatively low rotational speeds, a significant influence of speed on both excitation and displacement behavior is observed. It therefore appears reasonable to further investigate dynamic effects such as unbalanced excitations, gyroscopic forces, centrifugal forces, and to extend the range of rotational speeds considered.

6 Conclusion and outlook

By introducing an additional gear stage, stepped planetary gearboxes extend the inherent advantages of conventional planetary gear systems. They further enhance the power density and transmission ratio range of planetary gears. A deeper understanding of excitation behavior enables the development of quieter stepped planetary gearboxes and offers potential savings in tolerance design. Stepped planetary gearboxes are sensitive to axis misalignments, which can, however, be partially compensated by floating elements. Despite their advantages, stepped planetary gearboxes have been underexplored in the literature. Building on the work of Westphal et al. this paper addresses the need for further investigations [1].

This paper presents experimental investigations conducted on a stepped planetary gearbox test rig. The use of eccentric bushings enables the controlled application of defined misalignment states on the otherwise rigid gearbox. These modifications allow for the variation of the stepped planets axis alignment. However, manufacturing-induced misalignments of the carrier superimpose the effects of stepped planet misalignments, leading to varying contact conditions. As a result, the path of highest load shifts multiple times during a single carrier rotation. The resulting modulation effects, previously observed by Theling in planetary gearboxes, were for the first time identified in stepped planetary gearboxes as well [8]. The findings indicate that frequency modulations are less pronounced in the presence of planet pin position errors, suggesting that even with a floating sun gear, load imbalances still occur on the misaligned stepped planets. These modulation effects were observed in both transmission error and structure-borne noise, confirming that the measurement methodology itself is not the source of the observed modulations.

Additionally, the influence of rotational speed was examined. The results show that excitations at different orders can either be speed-dependent or speed-independent. Apart from the influence of axis misalignments, both the center displacement and the radial expansion of the sun gear trajectory were significantly affected by rotational speed, even at relatively low test speeds. Due to their high transmission ratio, stepped planetary gearboxes are well suited for high-speed applications, making their dynamic behavior particularly relevant. Future studies at higher speeds could provide insights into how dynamic effects such as unbalance excitations, gyroscopic and centrifugal forces influence the excitation and displacement behavior.

Acknowledgements The authors gratefully acknowledge financial support by the German Research Foundation (DFG) [501245855] for the achievement of the project results. The authors gratefully acknowledge financial support by the WZL Gear Research Circle for the achievement of the project results.

Funding Open Access funding enabled and organized by Projekt DEAL.

Conflict of interest M. Stary, C. Westphal and C. Brecher declare that they have no competing interests.

References

1. Westphal C, Brimmers J, Brecher C (2023) Influence of axis misalignments in stepped planetary gear stages on the excitation behavior—test rig development and simulative analysis. Forsch

Ingenieurwes 87:1103–1116. https://doi.org/10.1007/s10010-023-00709-z
2. Naunheimer H, Bertsche B, Ryborz J, Novak W, Fietkau P (2019) Fahrzeuggetriebe: Grundlagen, Auswahl, Auslegung und Konstruktion, 3rd edn. Springer Vieweg, Berlin, Heidelberg
3. Kampker A, Heimes HH (eds) (2024) Elektromobilität: Grundlagen einer Fortschrittstechnologie. Springer Nature, Berlin, Heidelberg
4. Syrnik R (2015) Untersuchung der fahrdynamischen Potenziale eines elektromotorischen Traktionsantriebs (Diss.). Technische Universität München, München
5. Schad N, Knödel U, Knoblauch D, Kreim A, Klostermann S (2009) Kompakte Antriebseinheit für Elektrostadtfahrzeuge—Aufbau, Wirkungsgrad, Akustik, Schaltstrategie. In: Institut für Maschinenelemente und Maschinengestaltung (IME). der RWTH Aachen University, Aachen
6. Müller HW (1998) Die Umlaufgetriebe: Auslegung und vielseitige Anwendungen, 2nd edn. Springer, Berlin
7. Klocke F, Brecher C (2017) Zahnrad- und Getriebetechnik: Auslegung—Herstellung—Untersuchung—Simulation, 1st edn. Hanser, München
8. Theling JA (2023) Auslegung von Planetengetrieben im elastischen Verzahnungsumfeld unter Berücksichtigung der Wechselwirkungen des Mehrfacheingriffes (Diss.). RWTH Aachen University, Aachen
9. Tsai S-J, Zhuang Q-Y (2023) Design and analysis of compound stepped planetary gear drives for better transmission performances. Forsch Ingenieurwes 87: 1037–1056. https://doi.org/10.1007/s10010-023-00702-6
10. Westphal C, Brimmers J, Brecher C (2023) Design of tooth flank modifications in transmission systems considering dynamic misalignments. In: The American society of mechanical engineers, editor. 2023 international power transmission and gearing conference. Boston, MA/USA, pp 20–23
11. Heider MK (2012) Schwingungsverhalten von Zahnradgetrieben: Beurteilung und Optimierung des Schwingungsverhaltens von Stirnrad- und Planetengetrieben (Diss.). TU München, München
12. Inalpolat M (2009) A theoretical and experimental investigation of modulation sidebands on planetary gear sets (Diss.). Ohio State University, Ohio
13. Wittke W (1994) Beanspruchungsgerechte und geräuschoptimierte Strinradgetriebe Toleranzvorgaben und Flankenkorrekturen (Diss.). RWTH Aachen University, Aachen
14. Iglesias M, Fernandez del Rincon A, de-Juan A, Garcia P, Diez-Ibarbia A, Viadero F (2017) Planetary transmission load sharing: manufacturing errors and system configuration study. Mech Mach Theory 111:21–38. https://doi.org/10.1016/j.mechmachtheory.2016.12.010
15. Singh A (2010) Load sharing behavior in epicyclic gears: physical explanation and generalized formulation. Mech Mach Theory 45:511–530. https://doi.org/10.1016/j.mechmachtheory.2009.10.009
16. Norm (2018) ISO 1328-1:2013: Definitionen und zulässige Werte für Abweichungen an Zahnflanken. Beuth
17. Neubauer B (2016) Lastverteilung und Anregungsverhalten in Planetengetriebensystemen (Diss.). TU München, München